Hybrid of Adaptive Response Surface methodology and Genetic Algorithm Monte Carlo Optimization method and Its Application in the Design of Moderator-Collimator for Accelerator based Thermal Neutron Radiography*

Chen-Xiao Yang,[1,2] Si-Ze Chen,[1,2,†] Lian-Xin Zhang,[2] Chuan Peng,[2,3] and Dan Xiao[2]

[1]Anhui University, Hefei, Anhui, 230601, China

[2]Hefei Institutes of Physical Science, Chinese Academy of Sciences, Hefei, Anhui, 230031, China

[3]University of Science and Technology of China, Hefei, Anhui, 230026, China

A new Monte Carlo (MC) neutronics optimization method named Hybrid of Adaptive Response Surface methodology and Genetic Algorithm Monte Carlo Optimization (HRG-MCO) is proposed to address the strong empirical dependence and low efficiency of global multi-parameter optimization in traditional neutronics design. HRG-MCO integrates the advantages of Response Surface Methodology (RSM) and Genetic Algorithm (GA). Specifically, neutron MC simulation results are iteratively utilized to adaptively construct an RSM model, ensuring the required accuracy. Subsequently, GA is employed to perform multi-parameter optimization based on the constructed RSM model, enabling the rapid determination of optimal design parameters. These optimized parameters are then fed back into the MC simulation model to derive the final design values. Comparative analysis with the traditional enumeration method and GA alone demonstrates the superior optimization efficiency of the proposed approach. To further validate its effectiveness, the method is applied to the optimization of a moderator-collimator system for a thermal neutron radiography system based on an accelerator. Two optimization tasks are performed: (1) determining the optimal efficiency under different source neutron energies and (2) optimization of thermal neutron photon yield ratio. The results highlight the efficiency and applicability of HRG-MCO in neutronics optimization design.

Keywords: Neutronics Design Optimization, Monte Carlo Simulation, Response Surface Methodology, Genetic Algorithm, Thermal Neutron Radiography

I. INTRODUCTION

In recent years, nuclear technologies based on neutron system such as advanced nuclear energy, boron neutron capture therapy (BNCT) and neutron radiography have developed rapidly. The advancement of these technologies heavily relies on the design and optimization of neutronics [1–5]. The Monte Carlo (MC) method is widely used in neutron system design due to its intuitive modeling and high computational accuracy [6]. However, traditional MC iterative optimization methods, which rely on enumeration or gradient-based approaches, require significant expertise from designers and struggle to balance multiple design factors and objectives leading to optimization results that lack systematic and global efficiency [7–13].

Genetic Algorithm (GA), with its powerful multi-parameter optimization capabilities, has been widely applied in MC design optimization in recent years. For example, in 2016, Hong-Quan Huang et al. proposed a method for estimating the parameters of typical overlapping nuclear pulse signals. First, the nuclear pulses are regarded as individual genes and the norm is set as the fitness function. Second, the global optimal solution is found by searching the population of genetic algorithm, so as to estimate the parameters of nuclear pulse [14]. In 2019, Byoungil Jeon et al. proposed an optimization method combining genetic algorithms with MC simulations to simultaneously calculate energy calibration parameters and gamma response functions [15]. In the same year, Guang Hu et al. optimized the structure of the moderator by using the output file of the neutron energy spectrum from MCNP5 as the objective function of the GA and solving for the maximum and minimum values of the objective function through GA [16]. In 2020, M.F. Yan et al. employed the genetic algorithm to optimize the structure of a fast neutron radiography system [17]. In 2022, S. Bagheri applied an intelligent method based on genetic algorithms, integrated with the MCNP program, to optimize the radiation shielding system of a small nuclear reactor, demonstrating higher optimization efficiency compared to traditional design methods [18]. In 2023, F. Cordella et al. combined genetic algorithms with MCNP6 and Geant4 for radiation shielding optimization [19]. Although the GA significantly improves optimization efficiency compared to the traditional enumeration method, its reliance on probabilistic sampling, mutation, and iterative adjustments can still lead to impractical computational times for large-scale, high-accuracy optimization problems or those with variable boundary conditions, especially when extensive MC simulations are required. Response Surface Methodology (RSM), on the other hand, optimizes by constructing multi-parameter function surface models and is currently

* This work was supported by the Nuclear Energy Development Project of China (No. [2019]1342) and the National Natural Science Foundation of China (No. U2341252).

† Corresponding author, size.chen@inest.cas.cn

another well-established multi-parameter optimization method. Due to the fast computational speed of function models, RSM offers high optimization efficiency. However, the accuracy of the RSM model construction directly impacts the final optimization results [20–24]. Therefore, building a high-accuracy RSM analysis model is key to the successful application of the RSM method.

This study attempts to combine the advantages of RSM and GA optimization techniques to establish a more efficient neutronic design optimization method. It is applied to the design of the moderator-collimator in a thermal neutron radiography system based on accelerator, aiming to address multiple design optimization challenges encountered in the process.

II. RESEARCH METHODS

A. Theory for the method

1. Monte Carlo simulation method

MC method is a computational technique based on probability and statistics, which approximates solutions to complex problems through random sampling. It leverages computer simulations of stochastic processes to obtain approximate solutions [25, 26]. The primary MC simulation software with neutron transport capabilities includes MCNP [27], OpenMC [28], and Geant4 [29].

In this study, the Geant4 software package is employed. Developed by CERN using C++ object oriented technology, Geant4 is a large-scale open source software package capable of simulating the physical transport processes of various particles, including neutrons, in matter. Due to its versatility and scalability, Geant4 has been widely applied across various fields, including nuclear technology applications.

To further improve the computational efficiency of neutron transport, this study also employs the Gamos extension package compatible with Geant4 to achieve geometry importance sampling acceleration [30].

2. Response Surface Methodology

RSM is a method that employs systematic experimental design to obtain data and uses a multivariate quadratic regression equation to model the functional relationship between influencing factors and response values [31]. By analyzing the regression equation, optimal parameter combinations can be identified, making it an effective approach for addressing multivariate optimization problems. The multivariate quadratic regression equation is expressed as:

$$y = \beta_0 + \sum_{i=1}^{n} \beta_i x_i + \sum_{i=1}^{n} \beta_{ii} x_i^2 + \sum_{i=1}^{n-1} \sum_{j=1}^{n} \beta_{ij} x_i x_j + \varepsilon \quad (1)$$

where y represents the predicted response value; β_0 denotes the regression intercept; β_i, β_{ii}, and β_{ij} correspond to the coefficients of linear, quadratic, and interaction terms, respectively; x_i and x_j are coded values of process variables; and ε accounts for residuals and experimental errors.

While conventional RSM typically employs second-order polynomials for surface fitting, higher-order polynomials may also be considered. However, higher-order models risk exhibiting unstable behavior in unexplored experimental regions and inherently require increased computational resources to enhance prediction accuracy [32]. The utilization of higher-order polynomials entails a greater number of unknown coefficients and enhanced functional complexity, thereby requiring meticulous evaluation of polynomial order to guarantee model reliability and accuracy.

In this study, given the requirements for optimized moderator-collimator system parameters and the semi-automated nature of the RSM process, the computational cost associated with implementing higher-order polynomials becomes negligible compared to the substantial resources required for MC simulations. Therefore, higher-order polynomial models with different orders are self-adopted for response surface analysis to achieve the target accuracy in system optimization.

3. Genetic Algorithm

GA is a computer algorithm designed for searching optimal solutions, characterized by its ability to directly manipulate structural objects, operate without reliance on derivatives or function continuity constraints, and exhibit implicit parallelism and global optimization capabilities. It adaptively adjusts search directions through probabilistic methods [33–35]. By simulating natural selection and genetic variation processes, GA intelligently explores solutions to complex problems. The algorithm maintains a diverse population and iteratively improves solution quality through operations such as selection, crossover, and mutation, enabling effective exploration of potential optimal regions in the solution space without requiring gradient information from the objective function [36].

In this study, the genetic algorithm was primarily employed to identify the extrema of the fitted function derived from response surface analysis, with a population size of 100, crossover probability of 0.5, mutation probability of 0.2, and 50 iterations. The optimization process was implemented using the classical genetic algorithm framework from the DEAP framework in Python.

B. Establishment of the proposed method

The proposed method, named Hybrid of Adaptive Response Surface methodology and Genetic Algorithm

Monte Carlo Optimization (HRG-MCO), utilizes Python to integrate response surface analysis algorithms, MC calculations, and GA, with its detailed optimization design workflow illustrated in Figure. 1.

The methodology initially employs Latin Hypercube Sampling (LHS) to select initial calculation points with the multi-dimensional design parameters. These points are subsequently input into the MC model to calculate the target parameters. The resulting data is then reintroduced into a multi-order function to fit RSM models of different orders. To validate the accuracy of the models, LHS is again utilized to sample test points for MC calculations. The relative error between the test point predicted values from the RSM model and the MC calculation values is calculated using Equation. 2 to assess the accuracy of the RSM model.

$$E = \frac{|y_1 - y_2|}{y_2} \times 100\% \tag{2}$$

Here, y_1 represents the predicted value, y_2 denotes the simulated value, and E represents the relative error between the two. This step ensures the reliability of the constructed RSM model for subsequent optimization processes. When the model accuracy falls below the preset accuracy criteria, the validation point data is reintroduced into the multi-order function fitting process to enhance the accuracy of the RSM model. Subsequently, new sampling points are extracted to revalidate the model accuracy. This iterative procedure is repeated until the validation accuracy of one of the response surface functions satisfies the system optimization design requirements. Based on the obtained RSM model, the GA is then employed to solve the multi-parameter optimization problem. Finally, the optimal parameter combination is reintroduced into the MC simulation to obtain the final results of the optimized system. This approach ensures a systematic and efficient optimization process with high accuracy.

C. Validation of the proposed method

In this study, a two-factor MC model was established based on the classical optimization problem of D-T neutron source moderation design to validate the effectiveness of HRG-MCO. A schematic diagram of the model is presented in Figure. 2. The model consists of two layers: (1) a tungsten multiplier layer with a diameter of 40 cm, and (2) a polyethylene moderation layer of the same diameter. The optimization range for both layers was confined to 1-20 cm. The neutron source is set as a point source with a radius of 1 cm, positioned 20 cm to the left along the central axis. A thermal neutron point detector was positioned at the center of the neutron exit surface of the moderation layer to record the thermal neutron flux below 0.5 eV resulting from the moderation process. For the initial and model validation phases, LHS was employed with 10 sample points in each case. The stopping criterion for the response surface model accuracy was set at 1%. The objective of the GA optimization was to maximize the thermal neutron flux at the point detector.

Figure. 3 shows the iterative computational results of the RSM modeling accuracy. The results indicate that after three iterations, 100 points validation error of the RSM model using a fourth-order polynomial reached 0.46%, which exceeds the predefined accuracy target of 1%. Based on this function model, the GA optimization was performed to determine the optimal parameters, which were identified as a neutron multiplier layer thickness of 10.8 cm and a moderation layer thickness of 5.5 cm. Under these parameter conditions, MC simulations yielded a thermal neutron moderation efficiency of 1.640×10^{-7} for the system.

To verify the efficiency of HRG-MCO and the accuracy of its optimization results, this study compares the outcomes obtained using HRG-MCO with those from the enumeration approach and the classical GA method. In the enumeration approach, calculations were performed with a thickness interval of 0.1 cm; for GA, comparisons were conducted under the same sampling conditions as HRG-MCO as well as under conditions with three times the sampling density. The comparative results are presented in Figure. 4 and Table. 1. Figure. 4 illustrates the comparison between the response surface model established by HRG-MCO (red) and that constructed via the enumeration method (blue), Where x_1 represents the multiplier layer thickness and x_2 represents the moderator layer thickness, showing good consistency between the two across various contour levels. Table. 1 details that the optimal value obtained from HRG-MCO using 40 samples deviates by only 0.49% from that obtained using 40,000 samples in the enumeration method. Under identical sampling conditions, the GA results deviate by 6.37% relative to the enumeration method, while the deviation is reduced to 0.73% under the triple sampling condition. These results indicate that HRG-MCO not only achieves significantly higher optimization efficiency compared to both the enumeration method and GA but also maintains a high degree of computational accuracy. Furthermore, as the optimization dimension increases, the growth in the number of sampling points further highlights the advantage of HRG-MCO in optimization efficiency compared to the traditional GA.

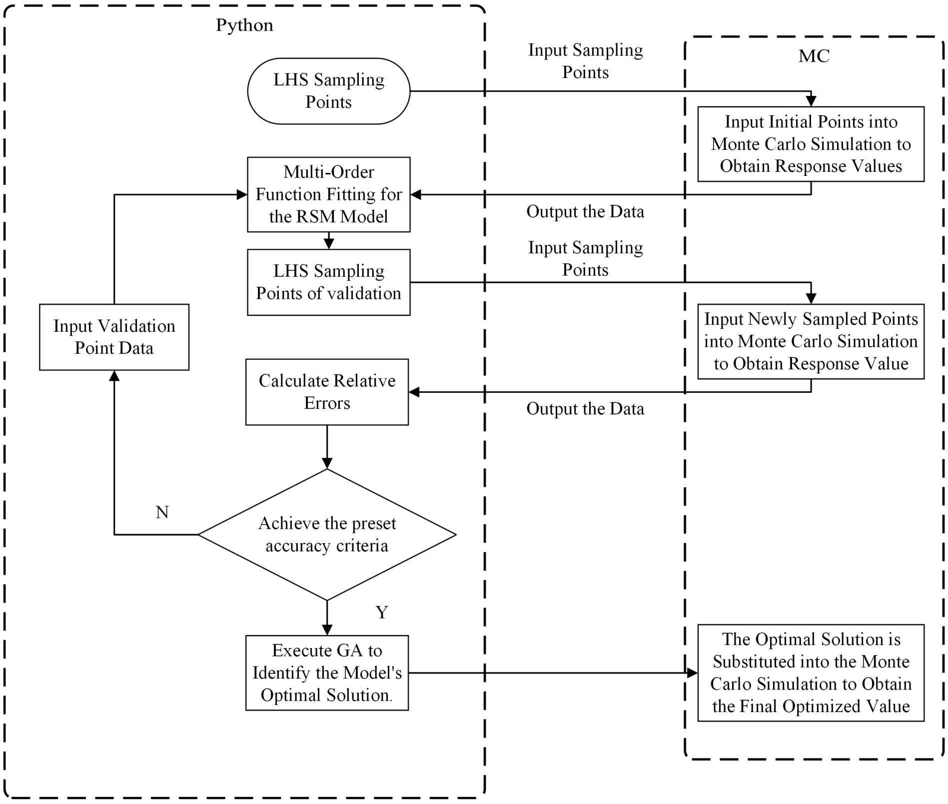

Fig. 1. Methodology flow chart of HRG-MCO.

TABLE 1. Comparison of results from different methods.

Method	Predicted Optimal Parameter (cm)	Thermal neutron moderation efficiency	Total Number of Sampling Points	Error (Relative to Enumeration Method)
Enumeration method	[10.8, 5.5]	1.648×10^{-7}	40000	/
HRG-MCO	[10.6, 5.4]	1.640×10^{-7}	40	0.49%
GA	[7.1, 6.4]	1.543×10^{-7}	40	6.37%
GA	[10.1, 5.4]	1.636×10^{-7}	126	0.73%

III. APPLICATION OF THE PROPOSED METHOD IN MODERATOR-COLLIMATOR DESIGN FOR COMPACT THERMAL NEUTRON IMAGING SYSTEMS

A. Study on moderation efficiency under different incident neutron energies

Compact thermal neutron radiography systems typically employ neutron sources based on an accelerator. Depending on the specific neutron-producing reaction channels or the accelerator beam energy, the energy of the source neutrons can be adjusted as required. Since the different source neutron energies will directly affect the thermal neutron moderation efficiency of the moderator collimator, determining the optimal moderation efficiency at different neutron energies is crucial for selecting the neutron source and accelerator beam energy in neutron radiography systems. However, under traditional methods, obtaining the neutron energy efficiency curve requires designing and optimizing the moderator-collimator for each individual energy point. This process makes it challenging to rapidly generate such a curve and even more challenging to conduct a quantitative assessment of the impact of various heavy metal multiplier materials on the optimal moderation efficiency curve.

To address the above issues, we conducted relevant research using HRG-MCO. First, an MC model of the moderator-collimator is established, with the cylindrical structure. Figure. 5 shows a cross-sectional view along the central axis, where the yellow region represents the heavy metal multiplication layer, the green region represents the polyethylene moderator layer, and the blue region represents the graphite reflector. The inner wall of the collimation channel is lined with a 1-mm thick thermal neutron shielding layer, while the outermost layer of the moderator-collimator is a 10-mm thick BC_4 thermal shield. In line with Section 2.3, a thermal neutron point detector is placed at a collimation ratio (L/D) of 10. A

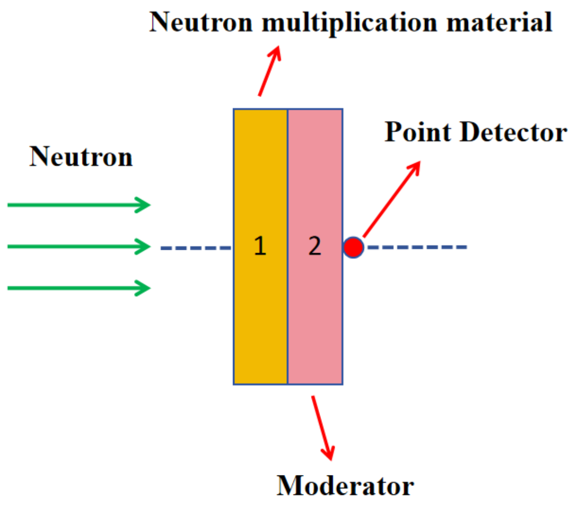

Fig. 2. (Color online) Structural diagram under two factors.

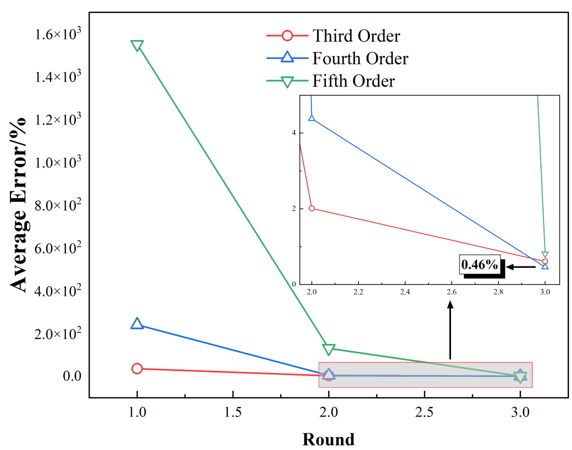

Fig. 3. (Color online) The relationship between the number of iterations and the average error of each order model in method validation.

mounting space for the accelerator target is reserved at the left entrance of the collimator. To enhance the general applicability of this research, no specific accelerator target room was modeled. Instead, the neutron source is defined as a planar source with a diameter of 20 mm, placed perpendicular to the moderator-collimator axis on the left side of the multiplication layer. In the figure, the parameters labeled 1 through 4 correspond to four optimization variables of the model: (1) the thickness of the front neutron multiplication layer, (2) the thickness of the outer neutron multiplication layer, (3) the thickness of the polyethylene moderator layer, and (4) the energy of the source neutrons. Since achieving the minimum neutron leakage rate would theoretically require an infinitely thick reflector and considering practical design constraints, the radial graphite reflector thickness is artificially set at 20.0 cm, while the axial graphite reflector thickness in the collimation zone is set at 39 cm.

For the design optimization calculation, both the initial LHS sampling and the verification sampling were performed with a sample size of 100 points, and the RSM model verification accuracy was set to 5%. Figure. 6 shows the final iterative calculation results for the RSM modeling verification accuracy. It can be observed that after five iterations, the verification accuracy of the eighth-order polynomial fit reached 4.96%, thereby achieving the targeted accuracy.

In order to obtain the optimal curve of neutron moderating efficiency varying with energy, different energy values were successively introduced into the established RSM model function at 0.5 MeV intervals within the 1-14 MeV energy region as the fitness function of GA optimization for each energy point. Then GA and MC methods were used to obtain the optimal design parameters and efficiency values for each energy point. Figure. 7 illustrates the variation in optimal moderation efficiency with energy (a) and the corresponding values of three optimized parameters (b) when W is used as multiplication material. It can be observed that in the 1-14 MeV energy range, the overall trend of the optimal thermal neutron moderation efficiency is a decrease followed by an increase as the incident neutron energy rises. A further comparison of the data trends in the two graphs reveals that the outer neutron multiplication layer becomes effective at lower source neutron energies compared to the forward neutron multiplication layer; however, the outer layer merely slows the rate of decline in thermal neutron moderation efficiency. In contrast, although the forward neutron multiplication layer only becomes active in the energy region above 6 MeV, its impact on thermal neutron moderation efficiency is significant. With the incorporation of the forward neutron multiplication layer, the thermal neutron moderation efficiency quickly increases.

To comparatively investigate the performance differences among multiplier layer materials including Pb, W, and depleted uranium (DU), the optimal moderation efficiency curves of Pb and DU were calculated using the aforementioned methodology, with the comparative results illustrated in Figure. 8. The optimized parameters of each material layer were systematically compared in Figure. 9. As clearly demonstrated in Figure. 8, DU exhibits significantly superior moderation efficiency compared to the other two materials. Figures . 9(a) and . 9(b) reveal that the enhanced performance of DU primarily stems from its lower energy threshold for neutron multiplication, enabling effective neutron generation at lower energy levels. Furthermore, Figure. 9(c) shows that the average energy of fast neutrons generated by DU and W multiplication is lower than that of Pb, indicating that a smaller moderator layer thickness is beneficial for improving neutron moderation efficiency.

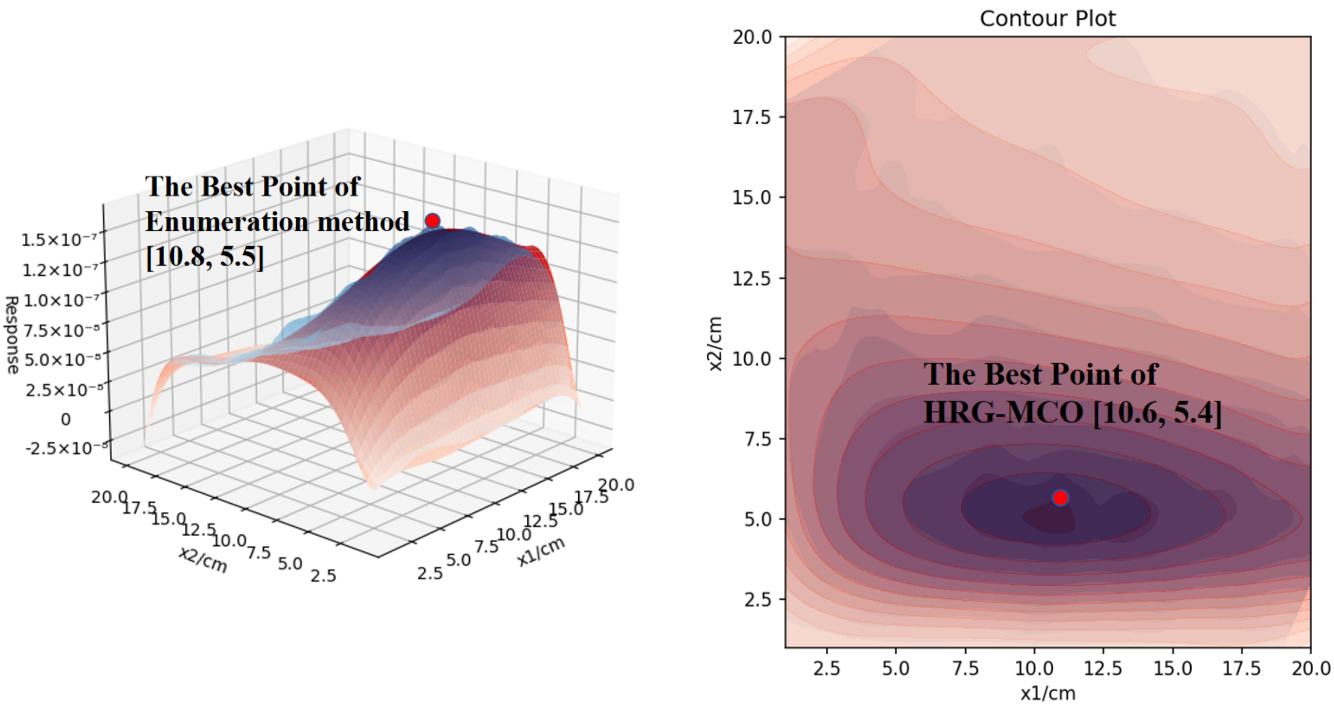

(a) (b)

Fig. 4. (Color online) (a) Three-dimensional response surface plot and (b) corresponding contour plot derived from two-factor validation and simulations.

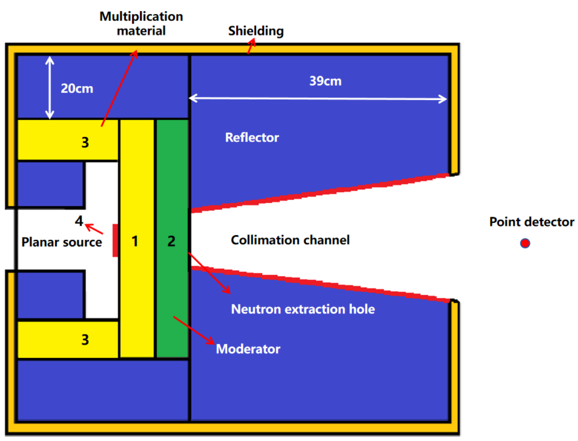

Fig. 5. (Color online) Structure of the Thermal Neutron Imaging System.

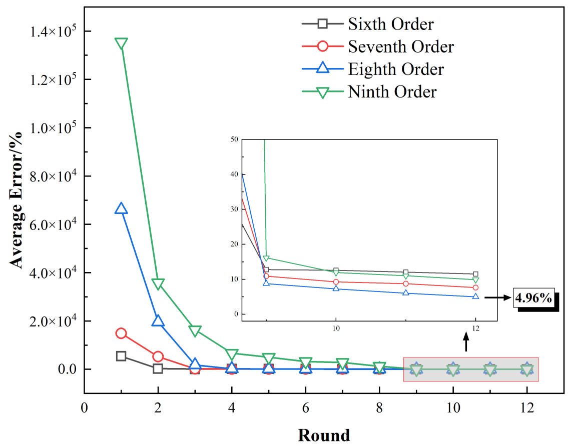

Fig. 6. (Color online) Results of RSM model accuracy verification in the energy optimal moderation efficiency problem.

B. Optimization of thermal neutron photon yield ratio

The combination of a conversion screen and an optical imaging system is the most commonly used imaging scheme in thermal neutron radiography systems. Due to the high energy of the neutrons in the accelerator source, the imaging quality is not only related to the emitted thermal neutron flux but also inevitably affected by the leakage of high-energy neutrons, which leads to the deterioration of imaging resolution. Therefore, maximizing the proportion of thermal neutron-induced photon yield in the conversion screen is another critical design optimization objective for the moderator-collimator system in accelerator-based thermal neutron radiography. However, an intrinsic trade-off exists between thermal neutron flux and photon yield ratio: increasing the photon yield ratio requires incorporating more high-energy neutron-absorbing materials, but their excessive

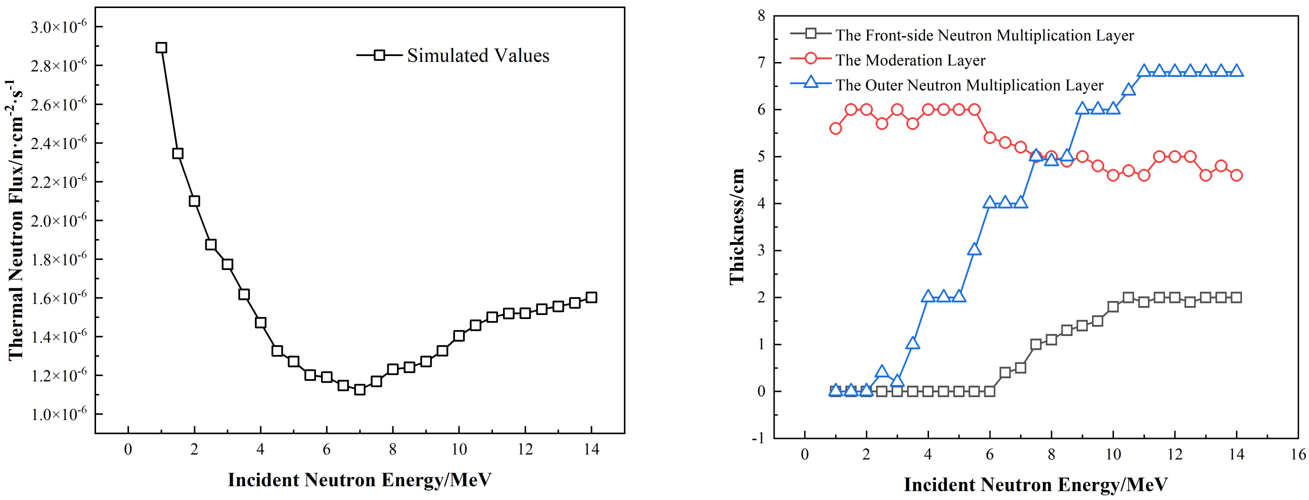

(a) (b)

Fig. 7. (Color online) (a) Variation curve of optimal moderation efficiency with energy; (b) Relationship between incident neutron energy and thickness parameters of key components.

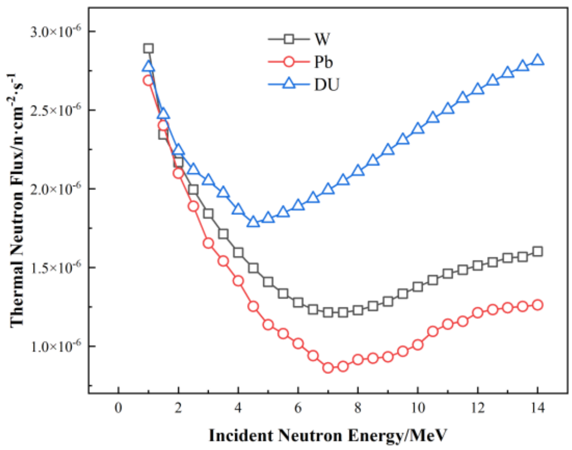

Fig. 8. (Color online) The variation curve of optimal moderation efficiency with energy for various multiplier materials.

use can negatively impact the transport efficiency of thermal neutrons. Using the newly developed optimization method, we investigate the photon yield optimization problem based on a D-T neutron source thermal neutron radiography model to enhance the performance of the imaging system.

Figure. 10(a) shows the variation curve of the photon yield of the ^{6}LiF/ZnS thermal neutron conversion screen as a function of neutron energy, as obtained from the authors' previous research [37]. Based on this curve, the impact of neutrons at different energy levels on photon yield can be assessed using the neutron energy spectrum from MC simulations of the moderator. As a preliminary study, to enhance computational efficiency, neutron energy is categorized into four energy regions: the thermal neutron region, epithermal neutron region, resonance neutron region, and fast neutron region, which are delineated in Figure. 10(a) with vertical dashed lines. The MC model adopts the same geometric configuration as in Figure. 5, with the neutron source energy fixed at 14.1 MeV from a D-T neutron source. W, a readily available material with moderate performance, is selected as the metal neutron multiplication layer. The thermal neutron point detector is replaced with a full-spectrum point detector, which records the flux proportions of neutrons emitted from the moderator-collimator within the four defined energy regions. The decision variables remain consistent with the first three variables in Section 3.1: the thickness of the front neutron multiplication layer (x_1), the thickness of the outer neutron multiplication layer (x_2), and the thickness of the polyethylene moderator layer (x_3). Figure. 10(b) illustrates the accuracy validation of the high-order RSM function. The results indicate that after three iterations, the sixth-order model is the first to meet the predefined 3% accuracy validation criterion.

To optimize the thermal neutron proportion, a GA fitness function was constructed as explicitly defined in Equation. 3:

$$F_5 = \frac{w_1 F_1}{w_1 F_1 + w_2 F_2 + w_3 F_3 + w_4 F_4} \tag{3}$$

$$\max F(x_1, x_2, x_3) = \begin{cases} \max F_1(x_1, x_2, x_3) \\ \max F_5(F_1, F_2, F_3, F_4) \end{cases}$$

$$\text{subject to} \begin{cases} 0 < x_1 \leq 20 \\ 0 < x_2 \leq 20 \\ 0 < x_3 \leq 20 \end{cases} \tag{4}$$

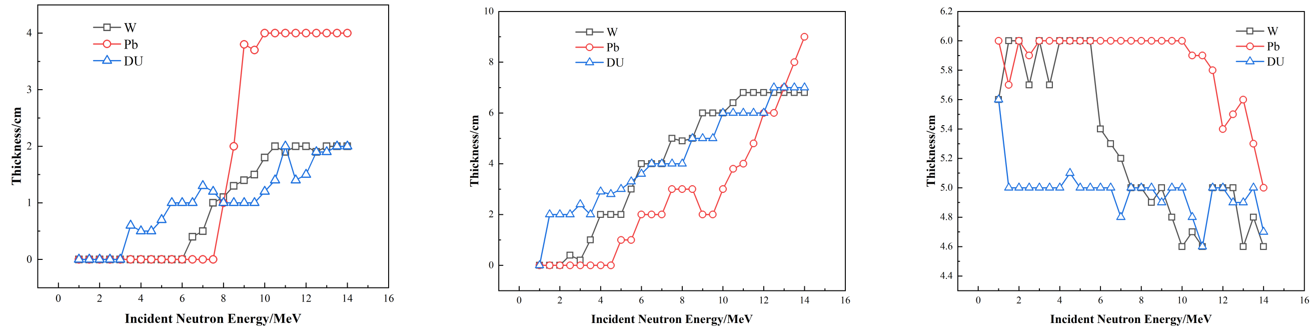

(a) (b) (c)

Fig. 9. (Color online) Comparison of optimized parameters for three multiplier materials: (a) front-side multiplier layer optimization, (b) outer multiplier layer, and (c) moderation layer.

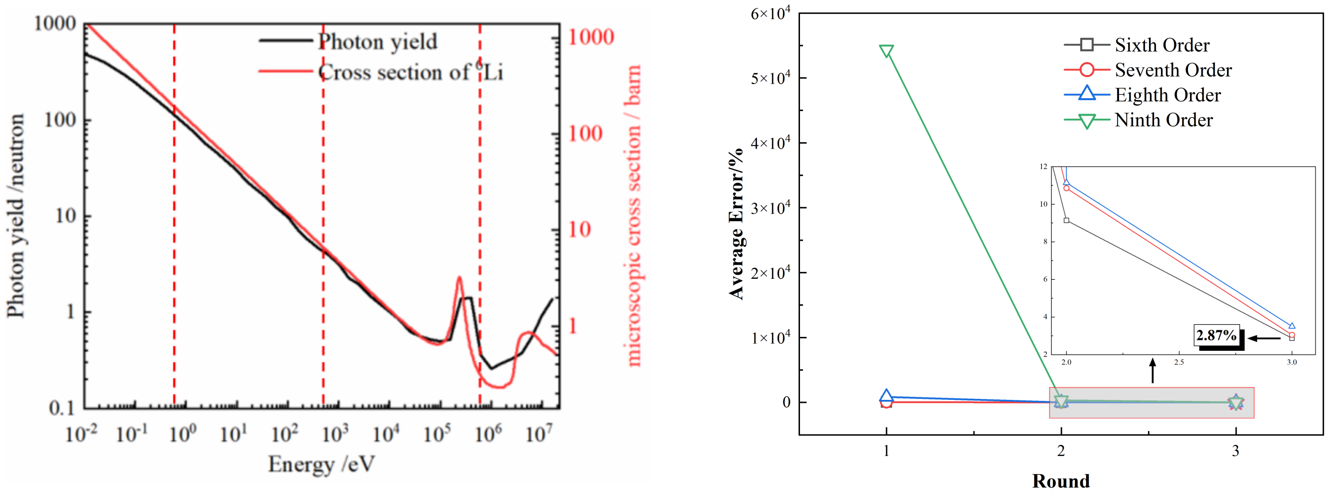

(a) (b)

Fig. 10. (Color online) (a)Relationship between photon yield and neutron energy [37] and (b) Accuracy verification results of the RSM modeling for the light yield optimization of the moderator-collimator system.

In the equation, F_5 represents the function that describes the proportion of thermal neutron photon yield relative to the total photon yield. The coefficients w_1 to w_4 correspond to the photon yield weights of thermal neutrons, epithermal neutrons, resonance neutrons, and fast neutrons, respectively, as determined from Figure. 10(a) and detailed in Table. 2. F_1 to F_4 represent the neutron flux rates in the four energy regions, calculated using the established RSM functions.

TABLE 2. Weighting factors for light yield across different energy regions.

Energy Region	W_1 (Thermal)	W_2 (Epithermal)	W_3 (Resonance)	W_4 (Fast)
Average Value	368.29	35.69	1.43	0.56
Normalization	0.907	0.088	0.004	0.001

Building on Equation. 3, the optimization constraint function for NSGA-II can be further established, as expressed in Equation. 4:

In this equation, F represents the overall objective function, with the optimization space for decision variables x_1 to x_3 constrained to the range of 0 to 20 cm. The parameters for the GA are set as follows: the parent population size (μ) is 100, the offspring population size (λ) is 200, the crossover probability is 0.5, the mutation probability is 0.2, and the maximum number of generations is 100. A blended crossover operator is employed, and Gaussian mutation is applied to balance solution diversity and convergence.

Figure. 11 presents the Pareto front solutions obtained through GA optimization. As shown in Figure. 11, a nonlinear inverse relationship exists between the optimal solutions of thermal neutron flux and its photon yield ratio. As the thermal neutron flux increases, the photon yield ratio decreases gradually. By analyzing the slope variation of the relationship curve, it is observed that when the photon yield ratio is below 90%, the decline in

thermal neutron flux due to an increase in the photon yield ratio is relatively gradual. However, once the photon yield ratio exceeds 90%, the decline rate of thermal neutron flux accelerates significantly.

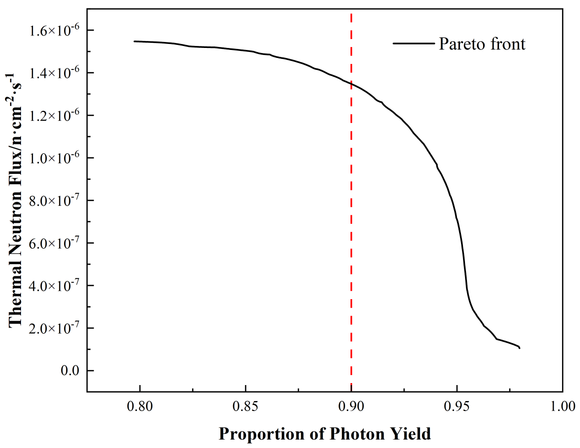

Fig. 11. (Color online) Pareto optimal solution sets.

The model parameters at a photon yield ratio of 90% (x_1 = 3.8 cm, x_2 = 5.6 cm, x_3 = 19.4 cm) were substituted into the MC model to recalculate the corresponding neutron energy spectrum, as shown in Figure. 12(a). Based on this spectrum, the photon yield distribution as a function of neutron energy was further computed, as illustrated in Figure. 9(b). The results indicate that non-thermal neutrons account for the largest proportion of the total neutron flux, reaching 61.9%. However, their contribution to photon production is minimal, making up only 0.61%. In contrast, although thermal neutrons represent only 8.2% of the total flux—less than a quarter of the total—they contribute up to 90.1% of the total photon yield.

IV. CONCLUSION

This study proposes a novel neutronics optimization design method that adaptively constructs a multi-order function model using RSM based on MC simulation results, followed by GA optimization. The proposed approach is applied to the design optimization of a moderator-collimator system for thermal neutron radiography. The key research findings are listed below:

1. By comparing the optimization results of HRG-MCO with those of the enumeration method and the traditional GA method for the neutron moderation problem of bilayer materials, the deviation of the results obtained using 40 sample points is only 0.49% compared to those obtained using 40,000 sample points in the enumeration method. Additionally, HRG-MCO outperforms the GA in optimization results under both the same sampling conditions and three times the sampling density.
2. An investigation of neutron moderation efficiency under varying incident neutron energies reveals that in the energy range of 1–14 MeV, the optimal moderation efficiency of the moderator-collimator initially decreases and then increases. Moreover, the efficiency ranking of W, Pb, and DU as neutron multiplication materials follows the order: DU > W > Pb.
3. Optimization of the conversion screen photon yield in a D-T neutron source-based thermal neutron radiography system reveals a nonlinear trade-off between thermal neutron flux and thermal neutron photon yield ratio. When the photon yield ratio exceeds 90%, the thermal neutron flux experiences a significant decline. At a photon yield ratio of 90%, the thermal neutron flux reaches approximately 85% of its maximum value.

The results of the above study demonstrate that the newly developed multi-objective parameter optimization method exhibits high design efficiency and accuracy in addressing multi-parameter optimization problems for the design of thermal neutron radiography moderator-collimators. Further validation and application in other neutronics fields, such as BNCT, will be conducted in the following study.

[1] Y.N. Zhu, Z.K. Lin, H.Y. Yu et al., "Study on the optimal incident proton energy of ^{7}Li(p, n)^{7}Be neutron source for boron neutron capture therapy," Nucl. Sci. Tech. 35, 60 (2024). doi: 10.1007/s41365-024-01420-6.

[2] Y. Zhang, C. Liu, S.L. Liu et al., "Prompt fission neutron uranium logging (II): dead-time effect of the neutron time spectrum," Nucl. Sci. Tech. 36, 19 (2025). doi: 10.1007/s41365-024-01615-x.

[3] Z.P. Qiao, Y.C. Hu, Q.X. Jiang et al., "Coin-structured tunable beam shaping assembly design for accelerator-based boron neutron capture therapy for tumors at different depths and sizes," Nucl. Sci. Tech. 34, 186 (2023). doi: 10.1007/s41365-023-01325-w.

[4] Y. Kiyanagi, "Neutron applications developing at compact accelerator-driven neutron sources," AAPPS Bull. 31, 1 (2021): 22.

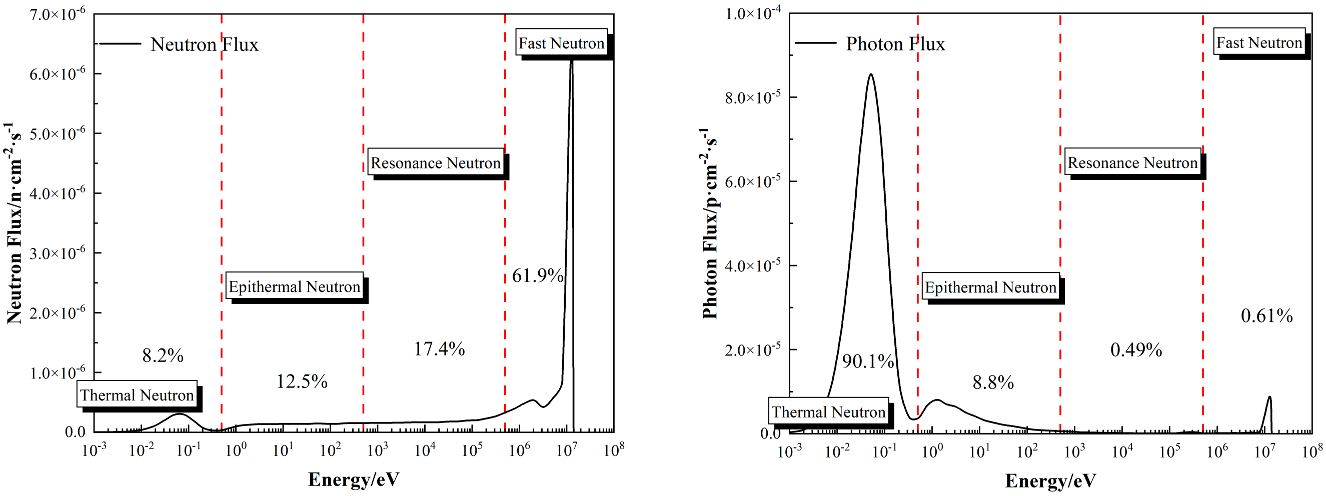

(a) (b)

Fig. 12. (Color online) (a) Neutron fluence rates across different energy intervals and (b) Photon yield distribution.

[5] Y. Sun, Q.B. Wang, P.C. Li et al., "Indirect neutron radiography experiment on dummy nuclear fuel rods for pressurized water reactors at CMRR," Nucl. Sci. Tech. 35, 189 (2024). doi: 10.1007/s41365-024-01534-x.

[6] P.F. Shen, X.D. Huo, Z.G. Li et al., "Mesh-free semi-quantitative variance underestimation elimination method in Monte Carlo algorithm," Nucl. Sci. Tech. 34, 14 (2023). doi: 10.1007/s41365-022-01156-1.

[7] Bai X., Ma J., Wei Z., et al., Development of a high-yield compact DD neutron generator. Nuclear Instruments and Methods in Physics Research Section A: Accelerators, Spectrometers, Detectors and Associated Equipment 2024, 169993.

[8] Iverson E. B., Enhancing neutron beam production with a convoluted moderator. Nucl. Instrum. Methods Phys. Res. Sect. A 762, 31–41 (2014).

[9] de Haan V., A high performance neutron moderator design. Nucl. Instrum. Methods Phys. Res. Sect. A 794, 122–126 (2015).

[10] Schönfeldt T., Advanced Neutron Moderators for the ESS (2016).

[11] Prastowo D., Design of Neutron Activation and Radiography Facilities Based on DD Generator. Indonesian Journal of Physics 34(2), 1-7 (2023). doi: 10.5614/itb.ijp.2023.34.2.1

[12] Li C., Jing S., Gao Y., Zhang W., MCNP optimization of fast neutron beam thermalization device based on D-T neutron generator. Fusion Engineering and Design 151, 111385 (2020). doi: 10.1016/j.fusengdes.2019.111385

[13] Li H., et al., Design of moderator and collimator for compact neutron radiography systems. Nuclear Instruments and Methods in Physics Research Section A: Accelerators, Spectrometers, Detectors and Associated Equipment 959, 163535 (2020).

[14] H.Q. Huang, X.F. Yang, W.C. Ding et al., "Estimation method for parameters of overlapping nuclear pulse signal," Nucl. Sci. Tech. 28, 12 (2017). doi: 10.1007/s41365-016-0161-z.

[15] Jeon B., Kim J., Moon M., Cho G., Parametric optimization for energy calibration and gamma response function of plastic scintillation detectors using a genetic algorithm. Nuclear Instruments and Methods in Physics Research Section A: Accelerators, Spectrometers, Detectors and Associated Equipment 930 (2019). doi: 10.1016/j.nima.2019.03.003

[16] Hu G., et al., A novel method for designing the moderator of accelerator-driven neutron source. Annals of Nuclear Energy 133, 96-99 (2019).

[17] Yan M. F., et al., Optimization design of a fast neutron imaging collimator by genetic algorithm. Journal of Instrumentation 15(12), P12002 (2020).

[18] Bagheri S., Khalafi H., SMR, 3D source term simulation for exact shielding design based on genetic algorithm. Annals of Nuclear Energy 191, 109915 (2023). doi: 10.1016/j.anucene.2023.109915

[19] Cordella F., Cappelli M., Ciotti M., et al., Genetic algorithm for multilayer shield optimization with a custom parallel computing architecture. Eur. Phys. J. Plus 139, 150 (2024). doi: 10.1140/epjp/s13360-023-04842-0

[20] Lamidi S., et al., Applications of response surface methodology (RSM) in product design, development, and process optimization. IntechOpen (2022).

[21] Sahoo P., Optimization of turning parameters for surface roughness using RSM and GA. Advances in Production Engineering & Management 6(3) (2011).

[22] Baligidad S. M., et al., RSM optimization of parameters influencing mechanical properties in selective inhibition sintering. Materials Today: Proceedings 5(2), 4903-4910 (2018).

[23] Ahmad A., Yadav A. K., Singh A., Process optimization of spirulina microalgae biodiesel synthesis using RSM coupled GA technique: a performance study of a biogas-powered dual-fuel engine. International Journal of Environmental Science and Technology 21(1), 169-188 (2024).

[24] Rahimi G., Chirlesan D., Soltani Z., Optimization of filler content and minimizing thickness of polymeric composite for shielding against neutron source by Response Surface Methodology (RSM) and Monte Carlo simulation. The European Physical Journal Special Topics

232(10), 1657-1663 (2023).
[25] Lux I., Monte Carlo Particle Transport Methods. CRC Press (1991). doi: 10.1201/9781351074834
[26] Z.P. Chen, A.K. Sun, J.C. Lei et al., "Multi-function and generalized intelligent code-bench based on Monte Carlo method (MagicMC) for nuclear applications," Nucl. Sci. Tech. 36, 57 (2025). doi: 10.1007/s41365-024-01626-8.
[27] Briesmeister J. F., MCNP-A general purpose Monte Carlo code for neutron and photon transport. Manual Version C (1986).
[28] Romano P. K., Horelik N. E., Herman B. R., et al., OpenMC: A state-of-the-art Monte Carlo code for research and development. Annals of Nuclear Energy 82, 90-97 (2015). doi: 10.1016/j.anucene.2014.07.048
[29] Agostinelli S., et al., GEANT4—a simulation toolkit. Nuclear Instruments and Methods in Physics Research Section A 506(3), 250-303 (2003).
[30] P. Arce, F. Sansaloni and J. Lagares, "Point Detector Scorer in GAMOS/Geant4," IEEE Nuclear Science Symposium & Medical Imaging Conference, Knoxville, TN, USA, 2010, pp. 1182-1184. doi: 10.1109/NSSMIC.2010.5873954.
[31] D.C. Montgomery, Design and analysis of experiments. Wiley, 2017.
[32] M.R. Rajashekhar, "A new look at the response surface approach for reliability analysis," Struct. Saf. 12, 3 (1993): 205-220.
[33] Z. Michalewicz and C.Z. Janikow, "GENOCOP: a genetic algorithm for numerical optimization problems with linear constraints," Commun. ACM 39, 12es (1996): 175-es.
[34] L. Davis, Genetic algorithms and simulated annealing, 1987.
[35] J.R. Sampson, Adaptation in natural and artificial systems (John H. Holland), 1976.
[36] K. Deb et al., "A fast and elitist multiobjective genetic algorithm: NSGA-II," IEEE Trans. Evol. Comput. 6, 2 (2002): 182-197.
[37] L.X. Zhang, S.Z. Chen, Z.D. Zhang et al., "Resolution analysis of thermal neutron radiography based on accelerator-driven compact neutron source," Nucl. Sci. Tech. 34, 76 (2023). doi: 10.1007/s41365-023-01227-x.